European Journal of Neuroscience, Vol. 26, pp. 925–934, 2007 doi:10.1111/j.1460-9568.2007.05731.x

Presynaptic protein distribution and odour mapping in glomeruli of the olfactory bulb of *Xenopus laevis* tadpoles

Ivan Manzini,[1,2] Stephan Heermann,[2,3] Dirk Czesnik,[1] Christoph Brase,[1] Detlev Schild[1,2] and Wolfgang Rössler[4]
[1]Department of Neurophysiology and Cellular Biophysics, University of Göttingen, Humboldtallee 23, 37073 Göttingen, Germany
[2]DFG Research Center for Molecular Physiology of the Brain (CMPB), University of Göttingen, Germany
[3]Department of Neuroanatomy, University of Göttingen, Kreuzbergring 36, 37075 Göttingen, Germany
[4]Department of Behavioural Physiology and Sociobiology, University of Würzburg, Am Hubland, 97074 Würzburg, Germany

Keywords: amino acids, calcium imaging, forskolin, immunocytochemistry, presynaptic proteins

Abstract

The sensory input layer in the olfactory bulb (OB) is typically organized into spheroidal aggregates of dense neuropil called glomeruli. This characteristic compartmentalization of the synaptic neuropil is a typical feature of primary olfactory centres in vertebrates and most advanced invertebrates. In the present work we mapped the location of presynaptic sites in glomeruli across the OB using antibodies to presynaptic vesicle proteins and presynaptic membrane proteins in combination with confocal microscopy. In addition the responses of glomeruli upon mucosal application of amino acid-odorants and forskolin were monitored using functional calcium imaging. We first describe the spatial distribution of glomeruli across the main olfactory bulb (MOB) in premetamorphic *Xenopus laevis*. Second, we show that the heterogeneous organization of glomeruli along the dorsoventral and mediolateral axes of the MOB is associated with a differential distribution of synaptic vesicle proteins. While antibodies to synaptophysin, syntaxin and SNAP-25 uniformly labelled glomeruli in the whole MOB, intense synaptotagmin staining was present only in glomeruli in the lateral, and to a lesser extent in the intermediate, part of the OB. Interestingly, amino acid-responsive glomeruli were always located in the lateral part of the OB, and glomeruli activated by mucosal forskolin application were exclusively located in the medial part of the OB. This correlation between odour mapping and presynaptic protein distribution is an additional hint on the existence of different subsystems within the main olfactory system in larval *Xenopus laevis*.

Introduction

The olfactory sensory organs of vertebrates are made of specialized neuroepithelia containing olfactory receptor neurons (ORNs) that project directly to the olfactory bulb (OB), where their axon terminals form synapses with the apical dendrites of the bulbar output neurons and local interneurons (Hálasz & Greer, 1993; Ennis *et al.*, 1996; Hildebrand & Shepherd, 1997; Mombaerts, 1999; Lledo *et al.*, 2005). Larval *Xenopus laevis* possess an olfactory organ consisting of two chambers, the principal cavity and the vomeronasal organ (Hansen *et al.*, 1998; Higgs & Burd, 2001). A third sensory chamber, the middle cavity, arises during metamorphosis (Hansen *et al.*, 1998; Higgs & Burd, 2001). The larval olfactory epithelium (OE) is exposed to water-borne odorants, and its ORNs have been shown to differentially respond to amino acids through a cAMP-independent transduction cascade (Vogler & Schild, 1999; Manzini *et al.*, 2002a,b; Manzini & Schild, 2003a, 2004; Czesnik *et al.*, 2006, 2007). Furthermore, recent calcium-imaging experiments have shown that amino acid stimuli are mapped on mitral and granule cells in the lateral OB, while ORNs using the cAMP transduction cascade activate those in the medial OB (Manzini *et al.*, 2002b; Czesnik *et al.*, 2003). In addition it has been shown that amino acid stimuli activate glomeruli in the lateral OB (Manzini *et al.*, 2007).

Correspondence: Dr I. Manzini, [1]Department of Neurophysiology and Cellular Biophysics, as above.
E-mail: imanzin@gwdg.de

Received 16 March 2007, revised 29 June 2007, accepted 2 July 2007

Axon terminals of ORNs synapse directly onto second-order neurons in the OB forming spheroidal structures called glomeruli. This typical organization of the sensory input layer of the OB is conserved in different species across phyla (Hildebrand & Shepherd, 1997; Rössler *et al.*, 2002; Lledo *et al.*, 2005). The organization of glomeruli, however, can differ markedly among species. Histological and electron microscopic investigations revealed that glomeruli in the OB of larval *Xenopus laevis* are organized rather loosely without defined periglomerular borders (Byrd & Burd, 1991; Nezlin & Schild, 2000; Nezlin *et al.*, 2003) and, unlike the general assumption that ORN axons project into one glomerulus each, ORNs of larval *Xenopus laevis* bifurcate upon entering the OB and project their axons into more than one glomerulus (Nezlin & Schild, 2005). Recently, by tracing the projections of axons from ORNs, Nezlin & Schild (2000) found a distinct organization of glomeruli in the ventral region of the main olfactory bulb (MOB), in contrast to a more plexus-like branching pattern of sensory axons in the dorsal part of the OB in premetamorphic *Xenopus laevis*. A similar heterogeneity in the organization of glomeruli was also found in the zebrafish (Baier & Korsching, 1994). It has also been shown that antibodies to synaptophysin, a synaptic vesicle-specific membrane protein (Jahn *et al.*, 1985), are an excellent tool to map the glomerular organization in larval *Xenopus laevis* (Nezlin *et al.*, 2003). Their spatial distribution in glomeruli within the different layers and subregions of the MOB of larval *Xenopus laevis*, however, has not been investigated up to now.

Here we used antibodies to the presynaptic vesicle proteins synaptophysin and synaptotagmin (Jahn *et al.*, 1985; Südhof *et al.*, 1987;

Brose *et al.*, 1992), as well as antibodies to the presynaptic membrane proteins syntaxin and SNAP-25 (Barnstable *et al.*, 1985; Blasi *et al.*, 1993) in combination with confocal microscopy to map the location of presynaptic sites in glomeruli across the OB. These proteins are associated with synaptic vesicles and the plasma membrane in presynaptic terminals (for general review, see Jahn & Südhof, 1994, 1999). In addition we monitored the responses of individual glomeruli upon mucosal stimulation with amino acid-odorants and forskolin using calcium imaging. The evaluation of the so-obtained data focused on the following points. First, how are glomeruli spatially distributed across the MOB in premetamorphic *Xenopus laevis*? Second, is the heterogeneity of glomeruli along the dorsoventral axis of the MOB associated with a differential distribution of presynaptic proteins? As a last point, by monitoring the amino acid- and forskolin-induced responses of glomeruli of the MOB, we asked whether there is a correlation between odour mapping and synaptic vesicle protein distribution.

Parts of this study have been reported previously in abstract form (Rössler *et al.*, 2001).

Materials and methods

Tissue preparation

Tadpoles of laboratory-bred *Xenopus laevis* (stages 49–54; staged after Nieuwkoop & Faber, 1994) were used for the experiments. The animals were cooled to complete immobility, and then killed by transection of the brain at its transition to the spinal cord. All procedures for animal handling and tissue dissections were carried out according to the guidelines of the Göttingen University Committee for Ethics in Animal Experimentation. A block of tissue containing the OE, the olfactory nerves and the brain was cut out and transferred in bath solution (see below). Brains were then immediately dissected out and transferred in 4% paraformaldehyde (PFA) in 0.1 M phosphate-buffered saline (PBS), pH 7.4, for at least 2 h at room temperature or overnight at 4 °C.

Immunocytochemistry

Antibodies to synaptophysin (polyclonal G113/p38 frog derived from rabbit), synaptotagmin I (monoclonal C41.1 from mouse), syntaxin 1 (HPC-1, monoclonal from mouse) and SNAP-25 (monoclonal from rabbit) were generously supplied by Dr Reinhard Jahn (Max Planck Institute for Biophysical Chemistry, Göttingen, Germany; Barnstable *et al.*, 1985; Jahn *et al.*, 1985; Südhof *et al.*, 1987; Brose *et al.*, 1992; Blasi *et al.*, 1993). C41.1 labelled a single band close to 66 kDa, G113/p38 labelled a double band at about 38 kDa, HPC1 labelled a single band close to 31 kDa and SNAP-25 labelled a single band below 31 kDa on Western blots of larval *Xenopus laevis* OB homogenate (data not shown). For immunocytochemistry, the PFA-fixed brains were washed in PBS and subsequently either sectioned on a Vibratome (Leica VT 1000S, Bensheim, Germany) or on a cryostat (Leica CM 1850). For slicing on the Vibratome the brains were embedded in 5% low-melting point agarose (Sigma, Deisenhofen, Germany) and sectioned at 70 μm. For preparation of cryosections the brains were submerged in 30% sucrose in PBS overnight for cryoprotection. The brains were then embedded in tissue-freezing medium (Reichert-Jung, Nussloch, Deutschland), sectioned on the cryostat at 20 μm and collected directly onto slides. Sections were then washed in PBS containing 0.2% Triton X-100 (PBST), and non-specific binding was blocked with 2% normal goat serum (NGS; ICN, Aurora, Ohio, USA) in PBST for 1 h at room temperature. Tissue was then incubated overnight at 4 °C with G113/p38frog (1 : 1000), C41.1 (1 : 500), HPC-1 (1 : 1000) and SNAP-25 (1 : 1000) diluted in 2% NGS/PBS. Primary antibody was washed off with PBS, and Alexa 488- or 546-conjugated goat anti-rabbit or mouse secondary antibodies (Molecular Probes, Leiden, the Netherlands) were applied at a dilution of 1 : 250 in 1% NGS/PBS for 2 h at room temperature. The secondary antibody was washed off in several changes of PBS. Slices were then mounted on slides in 80% glycerol/PBS.

Estimation of the number of glomeruli in the MOB

The number of glomeruli were counted in eight left or right OBs ($n = 5$ animals) stained with antibodies to synaptophysin (see above) serially sectioned on the cryostat at 20 μm. Counts per slice were corrected for double-counting in adjacent slices by dividing the result by $(1 + d/t)$, with d and t being the mean glomerulus diameter and the slice thickness, respectively (Weibel, 1979). Numbers of glomeruli are given as mean ± standard error of the mean (SEM).

Labelling of olfactory receptor axons with biocytin

Axons of ORNs were labelled with biocytin using the method described in more detail in Nezlin & Schild (2000). Briefly, to label receptor axons, the brains were pinned to the bottom of a silicone-covered Petri dish filled with bath solution, and the cut ends of the olfactory nerves were put on a small piece of filter paper presoaked in bath solution. A drop of paraffin oil was then placed onto the filter paper in order to isolate the filter paper from the bath. Then an aliquot of a solution containing (in mM): NaCl, 10; dimethylsulphoxide (DMSO), 1%; HEPES, 5, pH 7.2; biocytin, 1% (Molecular Probes) was pipetted onto the filter paper under the drop of paraffin. After 2–4 h of nerve filling, the brains were put in fresh bath solution for 2–4 h at 10 °C. Brains were then fixed in 4% PFA in PBS, pH 7.4, for at least 2 h at room temperature or overnight at 4 °C. For immunocytochemistry, the brains were further processed as described above. Biocytin-labelled sections were incubated for 2–3 h in Avidin Alexa 488 (Molecular Probes; 1 : 250 in PBS with 0.2% Triton X-100). Avidin was washed off in several changes of PBS.

Laser-scanning confocal microscopy

Preparations were viewed in a laser-scanning confocal microscope (Zeiss LSM 510) equipped with an inverted microscope (Zeiss Axiovert 100M), and both 15 mW argon and 1 mW helium/neon laser light sources, using appropriate filter combinations. Single and serial optical sections were imaged at intervals of 0.5–5 μm through the depth of the sections and saved as three-dimensional stacks. Images of single optical sections or two-dimensional projections were generated for each channel and merged with the use of pseudocolors. Where needed, the digitized images were modified only to enhance contrast, to merge images from consecutive sections of the same preparation, or to form montages of images from adjacent regions. Image processing and labelling of figures were performed with one or more of the following programs: Zeiss imaging software (Zeiss, Göttingen, Germany), Corel Photopaint and Corel Draw (Corel Corporation, Ottawa, Ontario, Canada).

Nose–brain preparation for confocal calcium imaging

Tadpoles of *Xenopus laevis* (stages 51–56; staged after Nieuwkoop & Faber, 1994) were killed as described above. A block of tissue containing the OE, the olfactory nerves and the anterior two-thirds of

the brain was cut out and kept in bath solution (see below). The tissue was glued onto the stage of a vibroslicer (VT 1000S, Leica, Bensheim, Germany) and only the dorsal surface of the OBs was sliced off. Thereby the cutting angle was chosen in a way to enter the OB straight above the olfactory nerve entrance. The OE were left intact. For a more detailed description of this preparation, see Czesnik *et al.* (2003). As at these stages well-developed glomeruli have been found only in the more ventral OB (Nezlin & Schild, 2000, 2005; Nezlin *et al.*, 2003), the above-described slicing technique ensures an ideal access to the glomerular layer. The more dorsal part of the OB consists of an apparently structureless fibre meshwork without any clear discernible glomeruli (Nezlin & Schild, 2000; present results). For calcium-imaging experiments the tissue slices were transferred to a recording chamber, and 200 μL of bath solution (see below) containing 50 μM Fluo-4/AM (Molecular Probes) was added. Fluo-4/AM was dissolved in DMSO (Sigma) and Pluronic F-127 (Molecular Probes). The final concentrations of Pluronic F-127 and DMSO did not exceed 0.1% and 0.5%, respectively. To avoid transporter-mediated destaining of neuropil of the OB (Manzini & Schild, 2003b), MK571 (Alexis Biochemicals, Grünberg, Germany), a specific inhibitor of the multidrug resistance-associated proteins (Gekeler *et al.*, 1995; Abrahamse & Rechkemmer, 2001), was added to the incubation solution. After incubation on a shaker at room temperature for 1 h, the nose–brain preparations were placed under a grid in a recording chamber (Edwards *et al.*, 1989) and placed on the microscope stage of an Axiovert 100M (Zeiss, Jena, Germany), to which a laser-scanning unit (LSM 510, Zeiss) was attached.

Calcium imaging of odour responses

Intracellular calcium ion concentrations were monitored using a laser-scanning confocal microscope (Zeiss LSM 510/Axiovert 100M). Fluorescence images (excitation at 488 nm; emission > 505 nm) of the OB were acquired at 1.27–5.1 Hz and 786–196 ms exposure time per image, with a number of images taken as control images before the onset of odour delivery. The fluorescence changes $\Delta F/F$ were calculated for glomerular clusters or individual glomeruli as $\Delta F/F = (F_1 - F_2)/F_2$, where F_1 was the fluorescence averaged over the pixels of a glomerular cluster or an individual glomerulus (regions of interest were outlined manually), while F_2 was the average fluorescence of that region of interest prior to stimulus application.

A response was assumed if the following two criteria were met: (a) the first two intensity values of the chosen region of interest $\Delta F/F\ (t_1)$ and $\Delta F/F\ (t_2)$ after stimulus arrival at the OE had to be larger than the maximum of the prestimulus intensities; and (b) $\Delta F/F\ (t_2) > \Delta F/F\ (t_1)$, with $t_2 > t_1$.

To obtain high-quality maps of the pixels in the recorded image sequences that showed odorant-induced responses (see Fig. 3), we analysed the data using a custom-written program in MATLAB (Mathworks, Natick, USA). A 'pixel correlation map' was calculated by cross-correlating the fluorescence signal of every pixel with that of its immediate neighbours, and then displaying the resulting value as a greyscale map. As physiological responses often give similar signals in adjacent pixels, this method specifically highlights those pixels. In contrast, pixels that contain only noise show uncorrelated traces and thus appear dark in the cross-correlation map.

Solutions and stimulus application

The composition of the bath solution was (in mM): NaCl, 98; KCl, 2; $CaCl_2$, 1; $MgCl_2$, 2; glucose, 5; Na-pyruvate, 5; HEPES, 10. The pH of the bath solution was adjusted to 7.8, which is the physiological pH in this poikilothermal species (Howell *et al.*, 1970). The osmolarity of the bath solution was 230 mOsmol. As odorants, we used a mixture of 15 amino acids (AAs, L-proline, L-valine, L-leucine, L-isoleucine, L-methionine, L-glycine, L-alanine, L-serine, L-threonine, L-cysteine, L-arginine, L-lysine, L-histidine, L-tryptophan, L-phenylalanine) applied either as a mixture of all 15 AAs, as submixtures or as single AAs (for details, see also Manzini *et al.*, 2007). Furthermore, we used forskolin as an activator of the adenylate cyclase. All chemicals were purchased from Sigma. The AAs were dissolved in bath solution (10 mM stock, each) and used at a final concentration of 200 μM. Forskolin was dissolved in DMSO (stock of 20 mM) and used at a final concentration of 100 μM. Stimulus solutions were prepared immediately before use by dissolving the respective stock solution in bath solution. The bath solution was applied by gravity feed from a storage syringe through a funnel drug applicator (Schild, 1985) to the recording chamber. The flow was 350 μL/min. Odorants were pipetted directly into the funnel without stopping the flow of the bath solution. The tip of the applicator was placed close to the ipsilateral OE. The dilution of the odorants within the funnel was less than 1%, the delay between the odorants leaving the funnel outlet and reaching the mucosal surface was less than 1 s, and after the end of stimulation odorants were completely rinsed from the mucosa within 15 s (for details, see Manzini *et al.*, 2002b). Outflow was through a syringe needle placed close to the OE to ensure that odorant molecules were removed rapidly. Direct effects of the AA stimuli on the OB were excluded by a series of control experiments. After stimulation with the mix of AAs, we cut the olfactory nerves and repeated the stimulation. We did not observe any responses to AA after transection of the olfactory nerves, and we found no differences from control conditions. The minimum interstimulus interval between odorant applications was at least 2 min.

Results

Glomerular organization in the MOB

We investigated the spatial distribution of glomeruli in the MOB using antibodies to synaptophysin as a marker for olfactory glomeruli. In larval *Xenopus laevis* synaptophysin-immunoreactivity (IR) is strongly associated with the glomerular layer (Nezlin *et al.*, 2003; Nezlin & Schild, 2005). Synaptophysin-IR and glomerular arborizations of ORN axons anterogradely stained with biocytin-avidin are clearly co-localized along the whole dorsoventral axis in the MOB of larval *Xenopus laevis* (Fig. 1A). Synaptophysin-IR was especially intense within glomeruli, indicating a high density of synaptic sites. The plexiform layer in the dorsal MOB was characterized by a more punctuated staining pattern, suggesting a more diffuse distribution of synapses. Very little or almost no labelling was detected in the interglomerular spaces. Generally, aggregations of synaptophysin-IR become gradually smaller and less distinct from the ventral to the dorsal OB. In addition, the density of synaptophysin-IR in the external plexiform layer clearly decreases from the ventral to the dorsal OB (Fig. 1A).

To investigate the detailed glomerular distribution in larval *Xenopus laevis* we examined the MOB from serial sections in the horizontal plane labelled with antibodies to synaptophysin. We consistently identified characteristic glomerular clusters in a mediolateral axis with borders that gradually changed along the dorsoventral axis of the MOB (Fig. 1B and C). The series of schematic drawings in Fig. 1B show that in the ventral part of the MOB glomeruli form four distinct clusters: a lateral cluster (lat); an intermediate cluster (int); a medial cluster (med); and a much smaller cluster (sc) in the most medial part

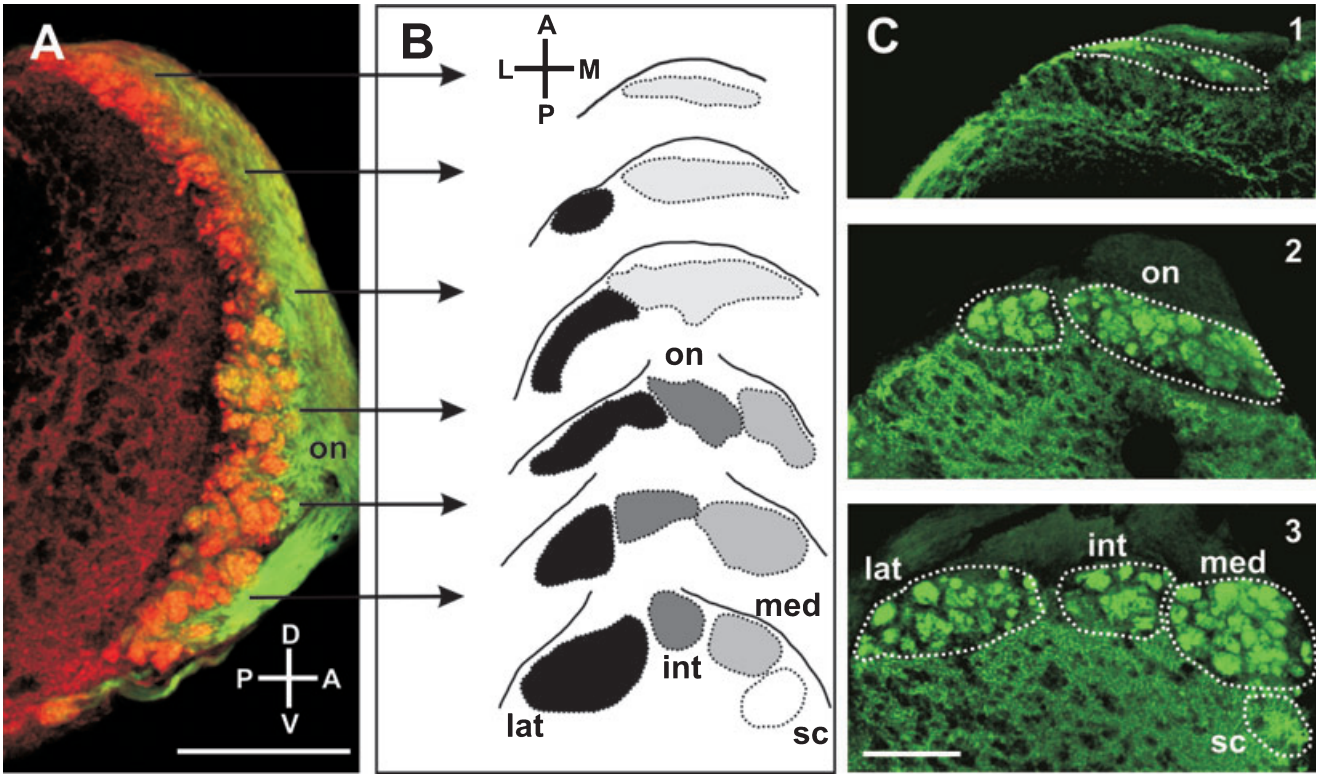

FIG. 1. Glomerular distribution in the MOB of larval *Xenopus laevis*. (A) Sagittal section of the MOB double-labelled with synaptophysin immunostaining (red) and anterograde labelling with biocytin through the olfactory nerve (green; on, olfactory nerve). The axes indicate: A, anterior; P, posterior; D, dorsal; V, ventral. (B) Schematic representation of the glomerular distribution in the MOB. The axes indicate: A, anterior; P, posterior; L, lateral; M, medial. Glomerular clusters: int, intermediate glomerular cluster; lat, lateral glomerular cluster; med, medial glomerular cluster; sc, small glomerular cluster. (C) Horizontal view of synaptophysin-immunolabelled sections of the anterior part of the MOB at three different heights (C1, dorsal OB; C2, intermediate OB; C3, ventral OB). Scale bars: 100 μm.

of the MOB (Fig. 1C, 3). While the smaller cluster disappears at the height of the nerve entrance, the three major groups still remain apparent and separate in the middle part of the MOB. In the more dorsal MOB the intermediate cluster fuses with the medial cluster forming a single and wider medial cluster (Fig. 1c, 2). Eventually, in the most dorsal MOB the lateral and medial clusters fuse into an elongated structure (Fig. 1C, 1). This principle distribution did not differ among stages 49–54 ($n = 15$ tadpoles).

As revealed by the double-labelling experiments described above, antibodies to synaptophysin consistently stained all glomeruli in larval *Xenopus laevis*. We took advantage of this fact and estimated the total number of glomeruli by counting glomeruli in serially cryosectioned MOBs stained with antibodies to synaptophysin ($n = 5$ tadpoles). The total number of glomeruli was: 175 ± 7 (lateral cluster); 71 ± 6 (intermediate cluster); 99 ± 8 (medial cluster); and 4 ± 0.6 (small cluster). These numbers sum up to a total of 349 ± 14 glomeruli in the MOB.

Differential distribution of presynaptic proteins in the MOB

Synaptophysin-IR was uniformly distributed within glomeruli in the MOB (Figs 1 and 2A). Similarly, also syntaxin-IR and SNAP-25-IR were equally distributed within glomeruli in the MOB (Fig. 2B and C). This equal distribution of syntaxin-IR and SNAP-25-IR within glomeruli of the MOB was consistently found in the OB of tadpoles of different stages ($n = 4$ and 5 tadpoles, respectively). Interestingly, synaptotagmin-IR revealed a different distribution in the glomerular layer of the MOB. Only glomeruli in the lateral and, to a lesser extent, in the intermediate cluster were labelled, whereas glomeruli in the medial cluster of the MOB were not or only very weakly labelled. This becomes particularly evident in preparations stained with synaptotagmin antibodies in which ORN axons were anterogradely traced with biocytin (Fig. 2D–F). The absence of synaptotagmin-IR in the medial cluster of glomeruli was consistently found in the OB of tadpoles of different stages ($n = 10$ tadpoles).

Calcium imaging of odour responses in glomeruli

The immunostaining experiments suggest a differential distribution of synaptic vesicle proteins in different regions of the MOB. While synaptophysin, syntaxin and SNAP-25 uniformly stained glomeruli in the whole MOB, an intense synaptotagmin staining was present only in glomeruli in the lateral and, to a lesser extent, in the intermediate cluster, and was almost absent in glomeruli in the medial cluster. As a first step to look at possible functional correlates we recorded odorant-induced responses of individual olfactory glomeruli of *Xenopus laevis* tadpoles upon mucosal application of amino acid odorants.

Figure 3A shows the OB of a nose–brain preparation stained with Fluo-4 (image acquired at rest). Application of a mixture of all amino acids to the intact ipsilateral OE induced changes of the calcium-dependent fluorescence in the glomerular layer, the mitral cell layer and the granule cell layer of the OB (Fig. 3B). Clearly, the amino acid-induced fluorescence changes occurred in the lateral half of the OB. The responding structures in the glomerular layer were located in the OB area of the lateral cluster of glomeruli. Mucosal amino acid application always led to a similar unilateral activation of the OB

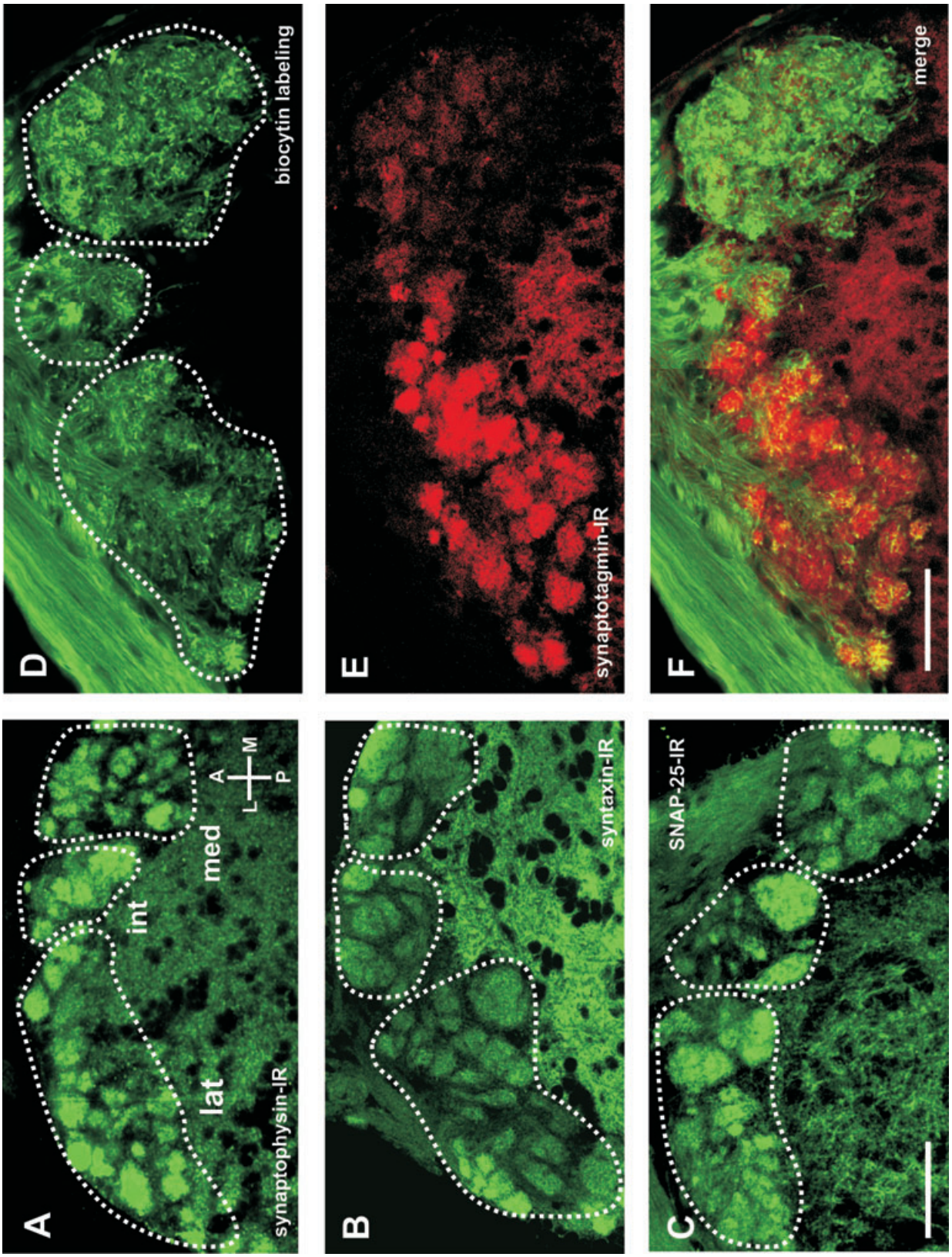

FIG. 2. Differential distribution of presynaptic proteins in the glomerular layer of the MOB. Horizontal sections of the MOB labelled with antibodies to synaptophysin (A), syntaxin (B) and SNAP-25 (C). All three antibodies label glomeruli in all glomerular clusters (int, intermediate glomerular cluster; lat, lateral glomerular cluster; med, medial glomerular cluster). The axes in (A) indicate: A, anterior; P, posterior; L, lateral; M, medial. (D) Horizontal section of the MOB anterogradely labelled with biocytin through the olfactory nerve. Double-staining of the olfactory receptor axons with biocytin in (D) clearly visualizes three glomerular clusters. (E) Synaptotagmin immunostaining of the same slice shown in (D). Synaptotagmin-immunoreactivity (IR) was limited to the lateral and partly to the intermediate glomerular cluster. (F) An overlay of the two channels (D and E) accents the unequal distribution of synaptotagmin-IR in the different clusters. Scale bars: 100 μm.

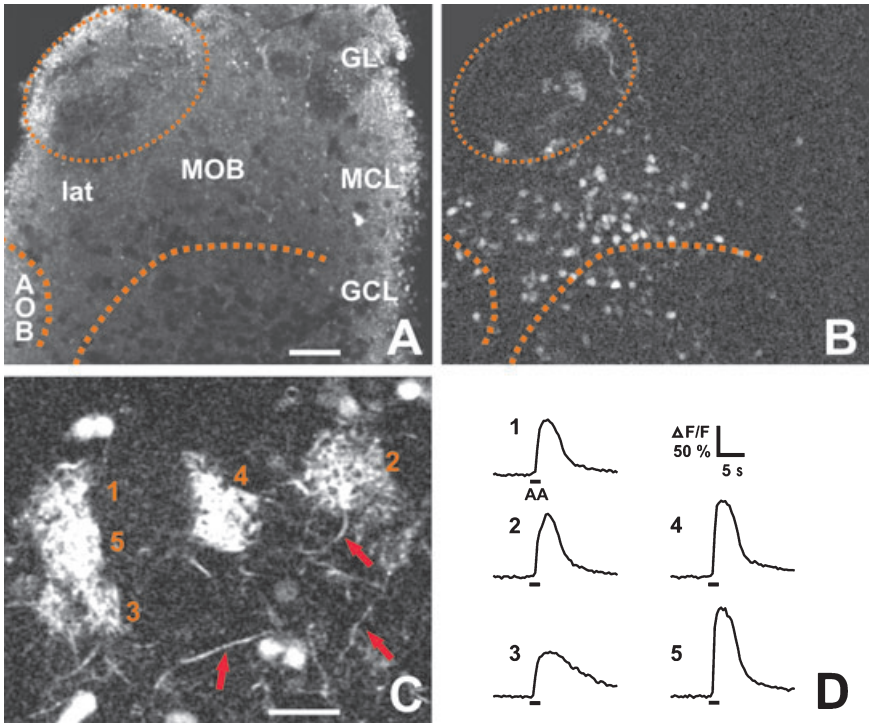

FIG. 3. Nose–brain preparation and amino acid-induced calcium signals in individual glomeruli in the lateral glomerular cluster of the MOB. (A) Fluo-4-stained OB of a nose–brain preparation. The dotted lines indicate the approximate borders of the accessory OB and the mitral and granule cell layer in the MOB and the position of the lateral glomerular cluster. The image was acquired at rest (AOB, accessory olfactory bulb; GCL, granule cell layer; GL, glomerular layer; lat, lateral glomerular cluster; MCL, mitral cell layer). (B) image of the same OB showing various glomeruli, mitral cells and granule cells activated by mucosal application of amino acids (200 μM). (C) higher magnification of the lateral cluster of another nose–brain preparation showing a number of amino acid-responsive glomeruli (see areas marked by numbers). The arrows indicate individual responsive fibres. (D) Time courses of the $[Ca^{2+}]_i$ transients of the five glomeruli indicated by numbers in (C). Scale bars: 50 μm (A); 20 μm (C).

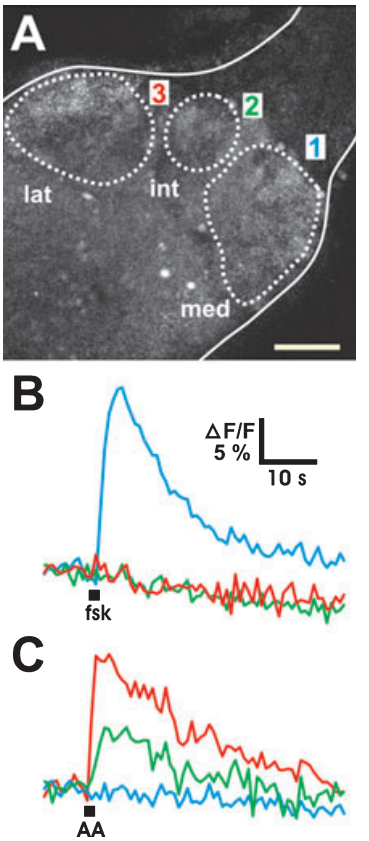

(n = > 100 tadpoles). To ascertain that the responding structures in the glomerular layer were individual glomeruli and not simply unstructured fibre meshwork, we imaged the glomerular layer of the OB at higher magnification. Figure 3C shows amino acid-induced fluorescence changes in glomeruli and processes in the OB area corresponding to the lateral cluster of glomeruli of a different nose–brain preparation. Clearly, individual glomeruli responded to application of the mixture of all amino acids to the ipsilateral OE (see numbers in Fig. 3C). Figure 3D shows the corresponding time courses of the $[Ca^{2+}]_i$ transient of these glomeruli. In 25 nose–brain preparations imaged with higher magnification and tested with the mixture of all amino acids we clearly identified 64 individual glomeruli that were activated upon mucosal amino acid stimulation. All of the responses were well beyond the minimum requirements for a response (see Materials and methods), and their amplitudes were markedly larger than the 5ó-range of prestimulus levels. Application of submixtures of the amino acids or individual amino acids did not change the results, except that, depending on the applied submixture

FIG. 4. Differential activation of glomerular clusters by amino acids and forskolin. (A) Fluo-4-stained OB of a nose–brain preparation (image acquired at rest). The dotted lines indicate the approximate borders of the three main glomerular clusters of the MOB (int, intermediate glomerular cluster; lat, lateral glomerular cluster; med, medial glomerular cluster). (B) Time courses of the $[Ca^{2+}]_i$ transients of the three glomerular clusters upon mucosal application of 100 μM forskolin (fsk; medial cluster: blue line; intermediate cluster: green line; lateral cluster: red line). (C) Time courses of the $[Ca^{2+}]_i$ transients of the three glomerular clusters upon mucosal application of 200 μM amino acids (same colours as in B). The entire clusters were taken as regions of interest. Scale bar: 100 μm.

or individual amino acid, only a subgroup of the amino acid-sensitive glomeruli was activated (data not shown). All of the amino acid-responsive glomeruli were located in the lateral OB, the area of the OB covering the lateral cluster or at most the lateral portion of the intermediate cluster of glomeruli. On the other hand, we never observed any amino acid-induced response of glomeruli in the medial cluster.

To verify that the medial cluster of glomeruli is functional using our preparation and our method of odorant delivery, we applied forskolin in a number of preparations in addition to amino acids to the intact OE. We chose forskolin because it is known that its mucosal application activates mitral and granule cells in the medial part of the OB (Manzini *et al.*, 2002b). As expected, in all of the tested animals mucosal application of forskolin activated glomeruli only in the medial part of the OB, corresponding to the medial cluster of glomeruli (Fig. 4A and B). The entire clusters were taken as regions of interest. Subsequent application of amino acids to the same nose–brain preparation activated glomeruli in the lateral and partly in the intermediate cluster (Fig. 4A and C). Virtually identical results were obtained in all of the nose–brain preparations tested with both stimuli ($n = 7$ animals; stages 51–54). We thereby never observed any response to amino acids in the medial glomerular cluster, nor did we find any response to forskolin in the lateral or intermediate glomerular cluster. The $[Ca^{2+}]_i$ signals of non-responding glomerular clusters either stayed constant or slightly decreased, presumably due to bleaching (Fig. 4B and C). On the other hand, all responses ($n = 42$; seven nose–brain preparations, three clusters per preparation, two trials per stimulus) were reproducible and showed steep $[Ca^{2+}]_i$ increases that clearly met our requirements for a response (see Materials and methods). Not unexpectedly, the absolute response amplitudes differed from preparation to preparation.

These experiments unambiguously demonstrated differential activation of the three glomerular clusters in individual nose–brain preparations.

The nose–brain preparation does not allow monitoring of odorant responses in the most ventral part of the OB. It was therefore not possible to check whether the small cluster of glomeruli in the very ventral part of the OB responded to amino acids or forskolin. Whenever we imaged odorant responses in very dorsal parts of the OB, amino acids or forskolin responses were no longer disjoint, and the whole glomerular area of the OB uniformly responded to either stimulus (data not shown).

Discussion

In the present study, we determined the spatial organization of glomeruli along the mediolateral and dorsoventral axis in the MOB of larval *Xenopus laevis.* Thereby, we clearly identified three main glomerular clusters that changed their appearance along the dorsoventral axis of the MOB. In addition a very small cluster, as previously described by Nezlin & Schild (2000), was found in the very ventral part of the MOB. In a second step we showed that immunoreactivity to various presynaptic proteins was differentially distributed within these glomerular clusters. While synaptophysin-IR, syntaxin-IR and SNAP-25-IR were equally distributed within glomeruli in the MOB, synaptotagmin-IR was found only in glomeruli in the lateral and, to a lesser extent, in the intermediate cluster. As a last point we found that the differential distribution of synaptotagmin-IR correlates with the mapping of odorants in glomeruli within the MOB.

In larval *Xenopus laevis* synaptophysin-IR has been shown to be strongly associated with the glomerular layer (Nezlin *et al.*, 2003). The size of individual glomeruli demarcated by synaptophysin-IR corresponds to the size of glomeruli revealed in previous tracing experiments (Nezlin & Schild, 2000), indicating that synaptic sites are distributed across the entire glomerulus (Nezlin & Schild, 2000; Nezlin *et al.*, 2003). In addition, double-labellings with antibodies to synaptophysin and biocytin backfills of the olfactory nerve showed that synaptophysin-IR is co-localized with glomerular arborizations of ORN axons in the whole glomerular layer of the OB of larval *Xenopus laevis* (Nezlin *et al.*, 2003). These experiments indicate that most if not all ORN nerve terminals in the OB are synaptophysin positive. However, it appears that this correlation can vary over brain areas, as it has been shown that in the cerebral cortex of rats only about half of the γ-aminobutyric acid (GABA)ergic axons are synaptophysin positive (Bragina *et al.*, 2007). Furthermore, it has been shown that the ventral region of the MOB contains distinct glomeruli, whereas the dorsal region of the OB is more or less aglomerular and ORN axons terminate in a plexus-like neuropil (Nezlin & Schild, 2000).

In the present study we extended the above observations and investigated the spatial glomerular organization within the MOB. We found that glomeruli in the most ventral part of the MOB are subdivided into four clearly demarcated clusters. Towards the dorsal MOB they gradually lose their integrity and eventually end in a band-like aglomerular formation in the most dorsal part of the MOB (see Fig. 1). The lateral cluster contains the highest number of glomeruli, followed by the medial cluster, the intermediate cluster and the small cluster. Thereby, the total number of 349 ± 14 glomeruli in the MOB determined in the present study exceeded the number calculated in a previous study (Nezlin & Schild, 2000) by about 100. This difference can be explained by the two different staining techniques used in the two studies. While in the previous study the glomeruli were stained by a nerve backfill with biocytin, in the present study the glomeruli were stained using immunostaining to synaptophysin. It is known that during the nerve filling procedure a certain number of axons may miss dye uptake. In addition, double-labelling with biocytin backfills showed that synaptophysin-IR demarcated glomerular borders much more distinct, especially in the more dorsal regions of the MOB containing very small glomeruli. These two factors may account for the lower number of glomeruli reported in the previous study.

The observed unequal distribution of glomeruli within the MOB confirmed the observations of the previous report of our group (Nezlin & Schild, 2000), and is in line with the knowledge that ORNs in *Xenopus laevis* tadpoles of the used stages project to the ventral MOB (Meyer *et al.*, 1996; Reiss & Burd, 1997). A division of ORN axons in various projection fields in the OB of larval *Xenopus laevis* has also been reported in a previous study, where the ORN axons were visualized employing DiI injections in the olfactory nerve and soybean agglutinin staining (Gaudin & Gascuel, 2005). While in mammals an obvious clustering of glomeruli is not apparent, glomeruli are clearly gathered in various clusters also in other aquatic species (sea lamprey, Frontini *et al.*, 2003; trout, Riddle *et al.*, 1993; zebrafish, Baier & Korsching, 1994). The functional meaning of such glomerular clustering has, however, not been elucidated so far.

We started to address this point by searching for molecular attributes that differ among the glomerular clusters and identified an inhomogeneous distribution of presynaptic proteins within the different glomerular clusters. While synaptophysin-IR, syntaxin-IR and SNAP-25-IR were uniformly distributed in the entire glomerular layer, synaptotagmin-IR was differentially distributed among the glomerular clusters. The lateral and, to a lesser extent, the intermediate cluster were clearly labelled, but almost no immunolabelling was detected in the medial cluster of glomeruli. It has been proposed that synaptophysin is involved in multiple aspects of

synaptic vesicle exo- and endocytosis (Brose *et al.*, 1992; Staple *et al.*, 2000; Valtorta *et al.*, 2004). Syntaxin and SNAP-25 are presynaptic membrane proteins essential for Ca^{2+}-regulated exocytosis (Hanson *et al.*, 1997; Hodel, 1998). Synaptotagmin I has been shown to function as a Ca^{2+} sensor for the regulated exocytosis of neurotransmitters (Augustine, 2001; Koh & Bellen, 2003; Tucker *et al.*, 2004). So far 16 different isoforms of synaptotagmin have been identified in various different species (Südhof, 2002; Craxton, 2004), and their number may additionally be enhanced by alternative splicing (Nakhost *et al.*, 2003; Craxton, 2004). One possible explanation for the variety of isoforms is that the synaptotagmins have diverged to sense different ranges of intracellular Ca^{2+} concentrations, thus allowing different cells, or even various compartments of an individual cell, to fuse with membranes at different intracellular Ca^{2+} concentrations (Burgoyne & Morgan, 1998). Various studies have shown that experimental modifications of presynaptic proteins in neurons may alter their synaptic activity (Rosahl *et al.*, 1995; Schoch *et al.*, 2001; Varoqueaux *et al.*, 2002; Washbourne *et al.*, 2002). The inhomogeneous expression of presynaptic proteins in the different glomerular clusters could therefore indicate differences in synaptic transmission at the respective synapses. The possibility that ORN axon terminals belonging to the different glomerular clusters express different isoforms of synaptotagmin can not be excluded but, even in this case, the main result would not change: The different glomerular clusters in the OB of larval *Xenopus laevis* feature a heterogeneous synaptic vesicle protein expression. This difference between ORN axons projecting to the different glomerular clusters suggests the existence of olfactory subsystems within the main olfactory system of larval *Xenopus laevis*. In recent work from our group it has been shown that the main OE of larval *Xenopus laevis* has at least two subtypes of ORNs with different transduction mechanisms and different odorant specificity (Manzini *et al.*, 2002b; Manzini & Schild, 2003a; Czesnik *et al.*, 2006). One subset is activated by amino acids in a cAMP-independent way, the second subset responds to pharmacological agents activating the cAMP cascade. The natural odorants of this second subset have not yet been identified. In order to show whether these ORN subtypes project to different glomerular clusters in a mutually exclusive manner we recorded responses of glomeruli of the MOB after stimulation of the OE with amino acids and forskolin, a pharmacological agent activating the adenylate cyclase that has already been successfully used in studies with *Xenopus laevis* ORNs (Manzini *et al.*, 2002b; Manzini & Schild, 2003a). The result that all glomeruli activated by mucosal application of amino acids were clearly located in the lateral or at most in the intermediate part of the MOB clearly shows that the subset of amino acid-responsive ORNs, which lack the cAMP-mediated transduction pathway, exclusively project to glomeruli of the lateral or the intermediate cluster (see Fig. 3). Interestingly, a striking analogy has been reported in the zebrafish olfactory system (Sato *et al.*, 2005). In zebrafish, microvillous ORNs lacking the cAMP transduction cascade project their axons exclusively to the lateral OB, whereas ciliated ORNs expressing components of the cAMP transduction cascade project to the medial part of the OB. Previous reports have shown that amino acids and nucleotides elicit activation of glomeruli in the lateral region of the zebrafish OB (Friedrich & Korsching, 1997, 1998), while bile acids, gonadal steroids and prostaglandins activate glomeruli in the medial region of the OB (Friedrich & Korsching, 1998). A virtually identical organization of the olfactory system has been described in the channel catfish (Hansen *et al.*, 2003). Inversely, in the sea lamprey olfactory system ORNs lacking G_{olf}, the G-protein involved in the cAMP transduction cascade, project to glomeruli in the medial OB (Frontini *et al.*, 2003).

As in zebrafish (Friedrich & Korsching, 1998; Sato *et al.*, 2005) and the channel catfish (Hansen *et al.*, 2003), larval *Xenopus laevis* ORNs with cAMP cascade project to the medial OB (medial cluster). In a previous study we have shown that application of forskolin to the intact ipsilateral OE induced responses in mitral and granule cells in the medial part of the OB (Manzini *et al.*, 2002b). This implies that ORNs with a cAMP transduction cascade project their axons to the medial cluster of glomeruli. It further shows that in our preparation the medial cluster of glomeruli is functional. To substantiate this observation, in the present study we repeated the above experiments using a different preparation and focused the attention to responses in the glomerular layer of the MOB. As expected, mucosal application of forskolin exclusively activated glomeruli in the medial glomerular cluster (see Fig. 4). Bile acids, gonadal steroids and prostaglandins are definitely promising groups of natural odorants for this second subset of ORNs owing the cAMP transduction cascade. While amino acids are thought to trigger arousal and feeding behaviours, bile acids, prostaglandins and steroids most probably elicit social and endocrine responses (Sorensen & Caprio, 1998). Although it is known that, similarly as in the zebrafish, the OE of larval *Xenopus laevis* has both microvillous and ciliated ORNs (Hansen *et al.*, 1998), it remains to be clarified whether ORNs of the two subsystems in *Xenopus laevis* bear microvilli or cilia. Two recent studies have shown that olfactory receptor-derived cAMP signals seem to be crucial for axonal convergence onto olfactory glomeruli in the OB (Imai *et al.*, 2006; Chesler *et al.*, 2007). This suggests that the axonal convergence of ORNs of the cAMP-independent olfactory subsystem in larval *Xenopus laevis* must have an alternative signal to determine the target destinations of ORN axons. This interesting question is also certainly worth to be investigated in future studies.

Taken together, the glomerular layer of the MOB of larval *Xenopus laevis* is organized in spatially distinct clusters that receive input from different subsets of ORNs with varying transduction mechanisms, odorant spectra and an unequal composition of presynaptic proteins. This strongly suggests that the main olfactory system of larval *Xenopus laevis* is made up of at least two diverse subsystems with different functional relevance possibly emerged at different points in the evolution of the olfactory system.

Acknowledgements

The authors thank Gudrun Federkeil and Josko Kuduz for excellent technical assistance, and Dr Reinhard Jahn for generous supply with antibodies. This work was supported by grants from the DFG Research Center Molecular Physiology of the Brain (CMPB) to D.S. and I.M.

Abbreviations

DMSO, dimethylsulphoxide; IR, immunoreactivity; MOB, main olfactory bulb; NGS, normal goat serum; OB, olfactory bulb; OE, olfactory epithelium; ORN, olfactory receptor neuron; PBS, phosphate-buffered saline; PBST, PBS containing 0.2% Triton X-100; PFA, paraformaldehyde.

References

Abrahamse, S.L. & Rechkemmer, G. (2001) Identification of an organic anion transport system in the human colon carcinoma cell line HT29 clone 19A. *Pflugers Arch.*, **441**, 529–537.

Augustine, G.J. (2001) How does calcium trigger neurotransmitter release? *Curr. Opin. Neurobiol.*, **11**, 320–326.

Baier, H. & Korsching, S. (1994) Olfactory glomeruli in the zebrafish form an invariant pattern and are identifiable across animals. *J. Neurosci.*, **14**, 219–230.

Barnstable, C.J., Hofstein, R. & Akagawa, K. (1985) A marker of early amacrine cell development in rat retina. *Brain Res.*, **35**, 286–290.

Blasi, J., Chapman, E.R., Link, E., Binz, T., Yamasaki, S., De Camilli, P., Südhof, T.C., Niemann, H. & Jahn, R. (1993) Botulinum neurotoxin A selectively cleaves the synaptic protein SNAP-25. *Nature*, **365**, 160–163.

Bragina, L., Candiracci, C., Barbaresi, P., Giovedi, S., Benfenati, F. & Conti, F. (2007) Heterogeneity of glutamatergic and GABAergic release machinery in cerebral cortex. *Neuroscience*, **146**, 829–840.

Brose, N., Petrenko, A.G., Südhof, T.C. & Jahn, R. (1992) Synaptotagmin – a calcium sensor on the synaptic vesicle surface. *Science*, **256**, 1021–1025.

Burgoyne, R.D. & Morgan, A. (1998) Calcium sensors in regulated exocytosis. *Cell Calcium*, **24**, 367–376.

Byrd, C.A. & Burd, G.D. (1991) Development of the olfactory bulb in the clawed frog, Xenopus laevis: a morphological and quantitative analysis. *J. Comp. Neurol.*, **314**, 79–90.

Chesler, A.T., Zou, D.J., Le Pichon, C.E., Peterlin, Z.A., Matthews, G.A., Pei, X., Miller, M.C. & Firestein, S. (2007) A G protein/cAMP signal cascade is required for axonal convergence into olfactory glomeruli. *Proc. Natl Acad. Sci. USA*, **104**, 1039–1044.

Craxton, M. (2004) Synaptotagmin gene content of the sequenced genomes. *BMC Genomics*, **5**, 43.

Czesnik, D., Kuduz, J., Schild, D. & Manzini, I. (2006) ATP activates both receptor and sustentacular supporting cells in the olfactory epithelium of *Xenopus laevis* tadpoles. *Eur. J. Neurosci.*, **23**, 119–128.

Czesnik, D., Rössler, W., Kirchner, F., Gennerich, A. & Schild, D. (2003) Neuronal representation of odourants in the olfactory bulb of *Xenopus laevis* tadpoles. *Eur. J. Neurosci.*, **17**, 113–118.

Czesnik, D., Schild, D., Kuduz, J. & Manzini, I. (2007) Cannabinoid action in the olfactory epithelium. *Proc. Natl Acad. Sci. USA*, **104**, 2967–2972.

Edwards, F.A., Konnerth, A., Sakmann, B. & Takahashi, T. (1989) A thin slice preparation for patch clamp recordings from neurones of the mammalian central nervous system. *Pflugers Arch.*, **414**, 600–612.

Ennis, M., Zimmer, L.A. & Shipley, M.T. (1996) Olfactory nerve stimulation activates rat mitral cells via NMDA and non-NMDA receptors in vitro. *Neuroreport*, **7**, 989–992.

Friedrich, R.W. & Korsching, S.I. (1997) Combinatorial and chemotopic odorant coding in the zebrafish olfactory bulb visualized by optical imaging. *Neuron*, **18**, 737–752.

Friedrich, R.W. & Korsching, S.I. (1998) Chemotopic, combinatorial, and noncombinatorial odorant representations in the olfactory bulb revealed using a voltage-sensitive axon tracer. *J., Neurosci.*, **18**, 9977–9988.

Frontini, A., Zaidi, A.U., Hua, H., Wolak, T.P., Greer, C.A., Kafitz, K.W., Li, W. & Zielinski, B.S. (2003) Glomerular territories in the olfactory bulb from the larval stage of the sea lamprey Petromyzon marinus. *J. Comp. Neurol.*, **465**, 27–37.

Gaudin, A. & Gascuel, J. (2005) 3D atlas describing the ontogenic evolution of the primary olfactory projections in the olfactory bulb of Xenopus laevis. *J. Comp. Neurol.*, **489**, 403–424.

Gekeler, V., Ise, W., Sanders, K.H., Ulrich, W.R. & Beck, J. (1995) The leukotriene LTD4 antagonist MK571 specifically modulates MRP associated multidrug resistance. *Biochem. Biophys. Res. Commun.*, **208**, 345–352.

Hálasz, N. & Greer, C.A. (1993) Terminal arborizations of olfactory nerve fibers in the glomerula of the olfactory bulb. *J. Comp. Neurol.*, **337**, 307–316.

Hansen, A., Reiss, J.O., Gentry, C.L. & Burd, G.D. (1998) Ultrastructure of the olfactory organ in the clawed frog, Xenopus laevis, during larval development and metamorphosis. *J. Comp. Neurol.*, **398**, 273–288.

Hansen, A., Rolen, S.H., Anderson, K., Morita, Y., Caprio, J. & Finger, T.E. (2003) Correlation between olfactory receptor cell type and function in the channel catfish. *J. Neurosci.*, **23**, 9328–9339.

Hanson, P.I., Heuser, J.E. & Jahn, R. (1997) Neurotransmitter release – four years of SNARE complexes. *Curr. Opin. Neurobiol.*, **7**, 310–315.

Higgs, D.M. & Burd, G.D. (2001) Neuronal turnover in the Xenopus laevis olfactory epithelium during metamorphosis. *J. Comp. Neurol.*, **433**, 124–130.

Hildebrand, J.G. & Shepherd, G.M. (1997) Mechanisms of olfactory discrimination: converging evidence for common principles across phyla. *Annu. Rev. Neurosci.*, **20**, 595–631.

Hodel, A. (1998) SNAP-25. *Int. J. Biochem. Cell. Biol.*, **30**, 1069–1073.

Howell, B.J., Baumgardner, F.W., Bondi, K. & Rahn, H. (1970) Acid-base balance in cold-blooded vertebrates as a function of body temperature. *Am. J. Physiol.*, **218**, 600–606.

Imai, T., Suzuki, M. & Sakano, H. (2006) Odorant receptor-derived cAMP signals direct axonal targeting. *Science*, **314**, 657–661.

Jahn, R., Schiebler, W., Ouimet, C. & Greengard, P. (1985) A 38,000 dalton membrane protein (p38) present in synaptic vesicles. *Proc. Natl Acad. Sci. USA*, **82**, 4137–4141.

Jahn, R. & Südhof, T.C. (1994) Synaptic vesicles and exocytosis. *Annu. Rev. Neurosci.*, **17**, 219–246.

Jahn, R. & Südhof, T.C. (1999) Membrane fusion and exocytosis. *Annu. Rev. Biochem.*, **68**, 863–911.

Koh, T.W. & Bellen, H.J. (2003) Synaptotagmin I, a Ca2+ sensor for neurotransmitter release. *Trends Neurosci.*, **26**, 413–422.

Lledo, P.M., Gheusi, G. & Vincent, J.D. (2005) Information processing in the mammalian olfactory system. *Physiol. Rev.*, **85**, 281–317.

Manzini, I., Brase, C., Chen, T.W. & Schild, D. (2007) Response profiles to amino acid odorants of olfactory glomeruli in larval *Xenopus laevis*. *J. Physiol.*, **581**, 567–579.

Manzini, I., Peters, F. & Schild, D. (2002a) Odorant responses of *Xenopus laevis* tadpole olfactory neurons: a comparison between preparations. *J. Neurosci. Meth.*, **121**, 159–167.

Manzini, I., Rössler, W. & Schild, D. (2002b) cAMP-independent responses of olfactory neurons in *Xenopus laevis* tadpoles and their projection onto olfactory bulb neurons. *J. Physiol.*, **545**, 475–484.

Manzini, I. & Schild, D. (2003a) cAMP-independent olfactory transduction of amino acids in *Xenopus laevis* tadpoles. *J. Physiol.*, **551**, 115–123.

Manzini, I. & Schild, D. (2003b) Multidrug resistance transporters in the olfactory receptor neurons of *Xenopus laevis* tadpoles. *J. Physiol.*, **546**, 375–385.

Manzini, I. & Schild, D. (2004) Classes and narrowing selectivity of olfactory receptor neurons of *Xenopus laevis* tadpoles. *J. Gen. Physiol.*, **123**, 99–107.

Meyer, D.L., Jadhao, A.G., Bhargava, S. & Kicliter, E. (1996) Bulbar representation of the 'water-nose' during Xenopus ontogeny. *Neurosci. Lett.*, **220**, 109–112.

Mombaerts, P. (1999) Seven-transmembrane proteins as odorant and chemosensory receptors. *Science*, **286**, 707–711.

Nakhost, A., Houeland, G., Castellucci, V.F. & Sossin, W.S. (2003) Differential regulation of transmitter release by alternatively spliced forms of synaptotagmin I. *J. Neurosci.*, **23**, 6238–6244.

Nezlin, L.P., Heermann, S., Schild, D. & Rössler, W. (2003) Organization of glomeruli in the main olfactory bulb of *Xenopus laevis* tadpoles. *J. Comp. Neurol.*, **464**, 257–268.

Nezlin, L.P. & Schild, D. (2000) Structure of the olfactory bulb in tadpoles of *Xenopus laevis*. *Cell Tiss. Res.*, **302**, 21–29.

Nezlin, L.P. & Schild, D. (2005) Individual olfactory sensory neurons project into more than one glomerulum in Xenopus laevis tadpole olfactory bulb. *J. Comp. Neurol.*, **481**, 233–239.

Nieuwkoop, P.D. & Faber, J. (1994) *Normal Table of Xenopus Laevis (Daudin).* Garland Publishing, New York.

Reiss, J.O. & Burd, G.D. (1997) Metamorphic remodeling of the primary olfactory projection in Xenopus: developmental independence of projections from olfactory neuron subclasses. *J. Neurobiol.*, **32**, 213–222.

Riddle, D.R., Wong, L.D. & Oakley, B. (1993) Lectin identification of olfactory receptor neuron subclasses with segregated central projections. *J. Neurosci.*, **13**, 3018–3033.

Rosahl, T.W., Spillane, D., Missler, M., Herz, J., Selig, D.K., Wolff, J.R., Hammer, R.E., Malenka, R.C. & Südhof, T.C. (1995) Essential functions of synapsins I and II in synaptic vesicle regulation. *Nature*, **375**, 488–493.

Rössler, W., Kuduz, J., Schürmann, F.W. & Schild, D. (2002) Aggregation of f-actin in olfactory glomeruli: a common feature of glomeruli across phyla. *Chem. Senses*, **27**, 803–810.

Rössler, W., Schild, D. & Kuduz, J. (2001) Distribution of synaptic vesicle proteins in the main and accessory olfactory bulb of *Xenopus laevis*. In Elsner, N. & Kreutzberg, G.W. (Eds), *Göttingen Neurobiology Report 2001. Proceedings of the 4th Meeting of the German Neuroscience Society 2001*, **Vol. II**, 28th Göttingen Neurobiology Conference. Georg Thieme, Stuttgart, p. 468.

Sato, Y., Miyasaka, N. & Yoshihara, Y. (2005) Mutually exclusive glomerular innervation by two distinct types of olfactory sensory neurons revealed in transgenic zebrafish. *J. Neurosci.*, **25**, 4889–4897.

Schild, D. (1985) A computer-controlled device for the application of odours to aquatic animals. *J. Electrophysiol. Techn.*, **12**, 71–79.

Schoch, S., Deak, F., Konigstorfer, A., Mozhayeva, M., Sara, Y., Südhof, T.C. & Kavalali, E.T. (2001) SNARE function analyzed in synaptobrevin/VAMP knockout mice. *Science*, **294**, 1117–1122.

Sorensen, P.W. & Caprio, J. (1998) Chemoreception. In Evans, D.H. (Ed.), *The Physiology of Fishes*, CRC, Boca Raton, pp. 251–261.

Staple, J.K., Morgenthaler, F. & Catsicas, S. (2000) Presynaptic heterogeneity: vive la difference. *News Physiol. Sci.*, **15**, 45–49.

Südhof, T.C. (2002) Synaptotagmins: why so many? *J. Biol. Chem.*, **277**, 7629–7632.

Südhof, T.C., Lottspeich, F., Greengard, P., Mehl, E. & Jahn, R. (1987) A synaptic vesicle protein with a novel cytoplasmic domain and four transmembrane regions. *Science*, **238**, 1142–1144.

Tucker, W.C., Weber, T. & Chapman, E.R. (2004) Reconstitution of Ca^{2+}-regulated membrane fusion by synaptotagmin and SNAREs. *Science*, **304**, 435–438.

Valtorta, F., Pennuto, M., Bonanomi, D. & Benfenati, F. (2004) Synaptophysin: leading actor or walk-on role in synaptic vesicle exocytosis? *Bioessays*, **26**, 445–453.

Varoqueaux, F., Sigler, A., Rhee, J.S., Brose, N., Enk, C., Reim, K. & Rosenmund, C. (2002) Total arrest of spontaneous and evoked synaptic transmission but normal synaptogenesis in the absence of Munc13-mediated vesicle priming. *Proc. Natl Acad. Sci. USA*, **99**, 9037–9042.

Vogler, C. & Schild, D. (1999) Inhibitory and excitatory responses of olfactory receptor neurons of *Xenopus laevis* tadpoles to stimulation with amino acids. *J. Exp. Biol.*, **202**, 997–1003.

Washbourne, P., Thompson, P.M., Carta, M., Costa, E.T., Mathews, J.R., Lopez-Bendito, G., Molnar, Z., Becher, M.W., Valenzuela, C.F., Partridge, L.D. & Wilson, M.C. (2002) Genetic ablation of the t-SNARE SNAP-25 distinguishes mechanisms of neuroexocytosis. *Nat. Neurosci.*, **5**, 19–26.

Weibel, E.R. (1979) *Stereological Methods*, **Vol. 1**, Practical Methods for Biological Morphometry. Academic Press, London.